BNL-69484-CP/LBNL-51828

ELECTRON-CLOUD MITIGATION IN THE SPALLATION NEUTRON SOURCE RING*

J. Wei†, M. Blaskiewicz, J. Brodowski, P. Cameron, D. Davino, A. Fedotov, P. He
H. Hseuh, Y.Y. Lee, H. Ludewig, W. Meng, D. Raparia, J. Tuozzolo, S.Y. Zhang, BNL
A. Aleksandrov, S. Cousineau, V. Danilov, S. Henderson, ORNL
M. Furman, LBNL; M. Pivi, SLAC; R. Macek, LANL, USA; N. Catalan-Lasheras, CERN

Abstract

The Spallation Neutron Source (SNS) accumulator ring is designed to accumulate, via H^- injection, protons of 2 MW beam power at 1 GeV kinetic energy at a repetition rate of 60 Hz [1]. At such beam intensity, electron-cloud is expected to be one of the intensity-limiting mechanisms that complicate ring operations. This paper summarizes mitigation strategy adopted in the design, both in suppressing electron-cloud formation and in enhancing Landau damping, including tapered magnetic field and monitoring system for the collection of stripped electrons at injection, TiN coated beam chamber for suppression of the secondary yield, clearing electrodes dedicated for the injection region and parasitic on BPMs around the ring, solenoid windings in the collimation region, and planning of vacuum systems for beam scrubbing upon operation.

INTRODUCTION

Electron-cloud effects are important, but incompletely understood phenomena. Effects that can severely limit the performance of high-intensity proton synchrotrons include trailing-edge tune-shift and resonance crossing, electron-proton instability, emittance growth and beam loss, increases in vacuum pressure, heating of the vacuum pipe, and interference with beam diagnostics. Similar to the Proton Storage Ring at Los Alamos (LANL), where a strong, fast transverse instability occurs when a threshold intensity is exceeded [2], the effects may limit the performance of the SNS accumulator ring [3, 4].

ELECTRON GENERATION

We classify electron production into the following categories: (1) electrons generated at the stripping foil in the injection region; (2) electrons generated at the surfaces of collimators and vacuum pipe due to the impact of lost protons; (3) electrons produced by beam-induced multipacting from the vacuum-pipe wall; and, (4) electrons produced around the ring from residual-gas ionization.

Injection stripping

During the H^- charge-exchange injection at 1 GeV beam energy, the stripped electrons with a kinetic energy of 545 keV and a power of 2 kW are collected by a water-cooled catcher (Fig. 1). These electrons backscatter from the catcher and the vacuum chamber, resulting in a high concentration of electrons with a broad energy spectrum. The injecting- and circulating-beams impacting on the foil produce secondary emission of electrons at tens of eV energy. The injecting- and circulating-beam also produce knock-on electrons at a high energy (up to several MeV). The stripping-foil, operating at a high temperature around 2000 K, emits thermionic electrons at low energy [5].

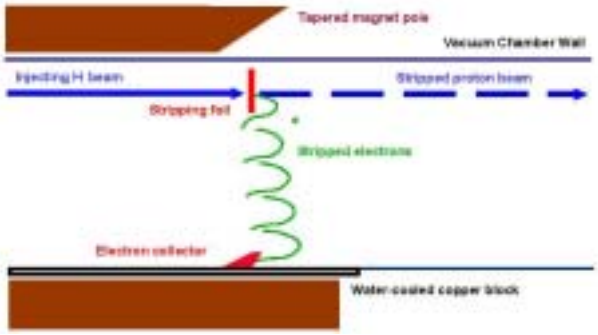

Figure 1: Injection area schematic layout.

Collimation region

The collimators are designed to collect more than 90% of the beam loss in the ring (Table 1). Protons incident on the collimator surfaces produce secondary electrons. Depending on the energy of the beam and the incident angle, the secondary electron-to-proton yield can greatly exceed 1 when the incident beam is nearly parallel to the surface [6]. Although a serrated surface reduces the generation of secondary-emission electrons, it is practically ineffective since protons incident on the front edge of the teeth easily escape from the collimator body due to the long proton stopping-length (about one meter) at 1 GeV energy.

Table 1: Estimated beam loss in the SNS ring of a 2 MW beam.

Mechanism	Location	Fraction	Power [W/m]
ring beam halo	collimator	1.9×10^{-3}	2×10^{3}
excited H^0 at foil	collimator	1.3×10^{-5}	20
energy straggling at foil	collimator	3×10^{-6}	4.5
H^- magnetic strip.	inj. dipole	1.3×10^{-7}	0.3
nucl. scatt. at foil	foil	3.7×10^{-5}	2.5
collimation ineff.	all ring	10^{-4}	0.9

*SNS is managed by UT-Battelle, LLC, under contract DE-AC05-00OR22725, DE-AC03-76SF00098, DE-AC03-76SF00515 for the U.S. Department of Energy. SNS is a partnership of six national laboratories: Argonne, Brookhaven, Jefferson, Lawrence Berkeley, Los Alamos, and Oak Ridge.

† jwei@bnl.gov

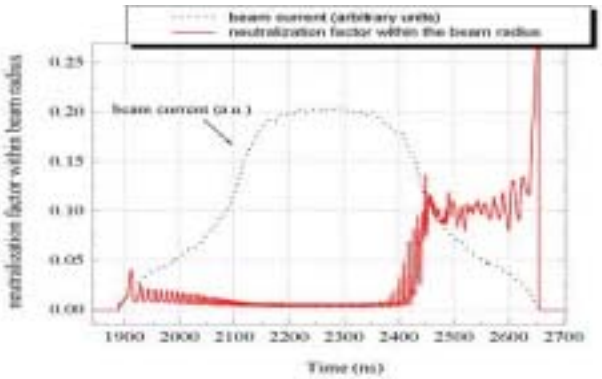

Figure 2: Computer simulation of electron generation in the SNS ring. The beam intensity is 2×10^{14} per bunch. The peak secondary-emission yield (SEY) is assumed to be 2. The peak neutralization level is about 10% within the proton rms beam radius, and about 100% on average within the beam pipe.

Beam-induced Multipacting

Beam-induced single-bunch, trailing-edge multipacting is likely to be the leading source of sustained electron-production [2, 7]. Electrons are attracted towards the rising edge of the proton bunch. At the trailing edge of the proton bunch, electrons are released and yet still accelerated by the bunch to multipact. The number of electrons grows exponentially at the trailing edge of the proton bunch. The energy gained by an electron is approximately [4]

$$\Delta E_e \approx 4 m_e c^2 \beta b \sqrt{\frac{r_e N_0}{s_b^3 B_f^3}} \qquad (1)$$

where N_0 is the number of protons in the bunch, s_b is the bunch separation, b is the pipe radius, and B_f is the bunching factor. For the SNS ring, $N_0 = 2 \times 10^{14}$, $s_b = 248$ m, $B_f \approx 0.5$, $b \approx 0.1$ m, and $\beta = 0.875$. The characteristic energy gain is approximately $\Delta E_e \approx 97$ eV. Single-bunch, trailing-edge multipacting is expected to occur (Fig. 2) [8].

Ionization

The rate of electron line-density increase per unit length of circumference is given by the relation

$$\frac{d^2\lambda_e}{dtds} = \frac{\rho_m \beta I \sigma_{ion} P}{e} \qquad (2)$$

where I is the beam current, σ_{ion} is the cross-section, P is in units of Torr. At the room temperature of 300 K, the molecular density ρ_m is about 3.3×10^{22} m^{-3}. For the SNS ring at a pressure of 10^{-8} Torr, a total number of 2.6×10^9 electrons is produced per turn when the proton intensity is 2×10^{14}. Residual gas ionization may feed these "seed" electrons to the trailing-edge multipacting process.

MITIGATION MEASURES

Control of the electron-cloud effects involves design consideration to minimize the beam loss, suppression of electron generation, and enhancement of Landau damping.

Low-loss design & operation

Minimization of beam loss is of primary importance [1]. Having a large transverse vacuum-pipe aperture and long, uninterrupted straight-sections are the two most important aspects considered. Collimators play an essential function in localizing the beam loss to controlled areas.

Landau-damping enhancement

A large vacuum-pipe aperture in high dispersion area and a large RF voltage provide sufficient momentum acceptance of $\pm1\%$ for a $480\pi\mu$m transverse acceptance. Longitudinal painting is used to expand the momentum spread of the injecting beam. Lattice sextupole families are used for chromatic adjustments, to either improve momentum acceptance or enhance damping. Octupoles are also available for a possible further enhancement.

Electron suppression

Injection area control Two chicane dipoles are special tapered to guide stripped electrons [9]. The electron collector is made of low charge-state C-C material with low backscattering yield.

Clearing electrodes A dedicated clearing electrode is implemented inside the stripping-foil assembly. A voltage up to 10 kV can be applied, adequate to suppress multipacting in the injection region. BPMs around the ring are designed to be also used as clearing electrodes capable of providing a voltage up to ±1 kV, overcoming the energy gain due to the proton bunch (Eq. 1, Fig. 3).

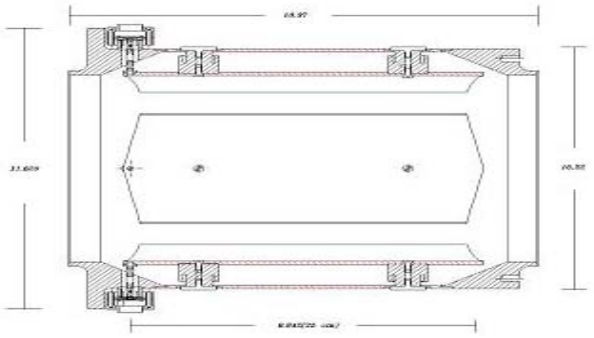

Figure 3: Floating-ground BPM for the SNS ring.

TiN surface coating The inner surface of the entire ring is coated with TiN. Coated chambers are tested for conductivity and rise-time response. With a variation within 20%, the thickness of 0.1 μm withstands the bombardment from electrons during the lifetime of the machine operation. For the ferrite of the extraction kicker inside the vacuum pipe, the coating pattern is selected to avoid Eddy-current heating and to prevent changes in material properties. Measurements of TiN-coated surfaces indicate a reduction of SEY by more than half of an unit (Fig. 4) [10]. Vacant ports are available for additional pumping if needed for the higher level of outgassing from the rougher coated

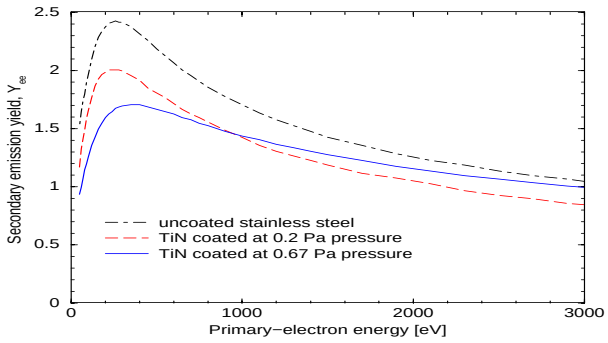

Figure 4: Secondary-electron yield for various coating conditions of the SNS ring chamber measured at CERN. Magnetron (dc) sputtering is used to coat the surfaces with 0.1 μm TiN. Surfaces coated at a pressure of 0.67 Pa, which has a lower peak Y_{ee} but a higher outgassing-rate comparing with those coated at a pressure of 0.2 Pa, are adopted.

surface. The present design does not allow NEG film coating which requires in-situ baking.

Solenoids Solenoids are planned for the vacant straights (about 5 m) in the collimation region to suppress electron multipacting. The solenoid field B_ϕ of about 50 G is strong so that the radius $r_\phi = m_e v_e / eB_\phi$ (12 mm for 300 eV electrons) of electron motion is small compared with the pipe radius. Effects on the proton beam can be minimized by alternating the polarities of the solenoids according to the betatron phase. Skew quadrupoles can further be used to correct the coupling.

Beam-in-gap cleaning In order to reduce the electrons trapped by the beam in the gap, the 250 ns beam gap is cleaned by a gap-cleaning kicker for the last 100 of the 1060-turn accumulation [11]. By resonantly exciting coherent betatron oscillations, beam residuals are driven into the primary collimator, where beam loss is measured with a gated fast loss monitor. The system uses MOSFET banks to supply pulses at 30 ns rise/fall time. The burst mode frequency, greater than 1 MHz, permits turn-by-turn kicking.

Chamber & vacuum Vacuum ports are screened, and steps in the vacuum pipe are tapered at 1-to-3 ratio to reduce peaked electric fields causing electron emission. A vacuum pressure of about 10^{-8} Torr ensures low electron generation from gas ionization.

Beam scrubbing Beam scrubbing at an electron dose level of 1 mC/mm^2 can further condition the vacuum surface during operations [12]. Vacant ports can house turbo pumps to function at a vacuum pressure above 10^{-6} Torr. Extended beam storage in the ring is planned to accelerate the scrubbing process.

Active damping The possibilities of mitigating the e-p instability with wideband resistive feedback are under investigation. The e-p instability results in coherent motion in the 100-200 MHz band with growth rates in the range 30-100 ms^{-1}. System gain of 0.1 is necessary to damp such large growth rates. A system is envisioned with 50 cm stripline kickers for each plane to achieve the high bandwidth and two pickups with flat response to 300 MHz having equivalent noise of less than 0.3 mm. The required gain is achieved with a 1.5 kW RF power amplifier driving each kicker.

Diagnostics & interference minimization

The stripping foils and the collector are monitored by the video systems. Five electron detectors are distributed at crucial locations around the ring.

Efforts are made to minimize the interference from the electron cloud. For example, the multi-channel plates for electron collection in the ring ionization profile monitors are recessed from the vacuum-chamber wall, and sweeping electrodes used to avoid superfluous signals.

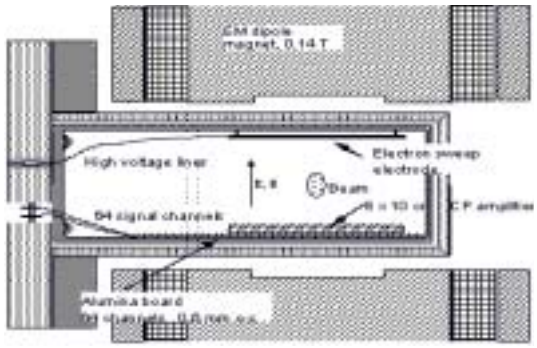

Figure 5: Ring IPM with sweeping electrodes, and with the multi-channel plates for electron collection recessed from the vacuum-chamber wall to avoid superfluous signals (courtesy R. Connolly).

SUMMARY

Present studies indicate that with preventive measures adopted to suppress electron generation and to enhance Landau damping, the impact of electron cloud can be minimized in the operation of the SNS ring.

We are indebted to the SNS team and collaborators, especially O. Gröbner, N. Hilleret, M. Plum, F. Ruggiero, N. Simos, P. Thieberger, R. Todd, F. Zimmermann.

REFERENCES

[1] J. Wei et al., PRST-AB **3** (1999) 080101; these proceedings; J. Wei, Rev. Mod. Phys. (Oct. 2003).
[2] R. Macek, Workshop Two-Stream Instab. Sante Fe (2000).
[3] M. Blaskiewicz et al, PRST-AB **6** (2003) 104203;these proc.
[4] J. Wei, R. Macek, ECLOUD'02, CERN-2002-001 (2002).
[5] M. Plum et al., PAC95 (1995) 3403.
[6] P. Thieberger et al., Phys. Rev. **61** (2000) 042901.
[7] V. Danilov et al., AIP Conf. Proc. 496 (N.Y. 1999), p. 315.
[8] M. Pivi, M. Furman, PRST-AB, **6** (2003) 034201.
[9] D. Abell et al., EPAC00, p. 2107 (2000).
[10] P. He et al., sub. to J. Vac. Sci. Tech. (2003); these proc.
[11] R. Witkover et al., PAC99 p. 2250; N. Catalan-Lasheras et al., PRST-AB **4** (2001) 010101.
[12] S.Y. Zhang et al., these proceedings.